OPEN ACCESS

TRANSPARENT PROCESS

molecular systems biology

Targeted proteomics reveals strain-specific changes in the mouse insulin and central metabolic pathways after a sustained high-fat diet

Eduard Sabidó[1], Yibo Wu[1], Lucia Bautista[1], Thomas Porstmann[1], Ching-Yun Chang[2], Olga Vitek[2,3], Markus Stoffel[1,*] and Ruedi Aebersold[1,4,*]

[1] Department of Biology, Institute of Molecular Systems Biology, ETH Zürich, Zürich, Switzerland, [2] Department of Statistics, Purdue University, West Lafayette, IN, USA, [3] Department of Computer Science, Purdue University, West Lafayette, IN, USA and [4] Department of Science, Faculty of Science, University of Zürich, Zürich, Switzerland
* Corresponding authors. M Stoffel or R Aebersold, Department of Biology, Institute of Molecular Systems Biology, ETH Zürich, Wolfgang-Pauli-Strasse 16, 8093 Zürich, Switzerland. Tel.: +41 44 633 4560; Fax: +41 44 633 1362; E-mail: stoffel@imsb.biol.ethz.ch or Tel.: +41 44 633 1071; Fax: +41 44 633 1051; E-mail: aebersold@imsb.biol.ethz.ch

The metabolic syndrome is a collection of risk factors including obesity, insulin resistance and hepatic steatosis, which occur together and increase the risk of diseases such as diabetes, cardiovascular disease and cancer. In spite of intense research, the complex etiology of insulin resistance and its association with the accumulation of triacylglycerides in the liver and with hepatic steatosis remains not completely understood. Here, we performed quantitative measurements of 144 proteins involved in the insulin-signaling pathway and central metabolism in liver homogenates of two genetically well-defined mouse strains C57BL/6J and 129Sv that were subjected to a sustained high-fat diet. We used targeted mass spectrometry by selected reaction monitoring (SRM) to generate accurate and reproducible quantitation of the targeted proteins across 36 different samples (12 conditions and 3 biological replicates), generating one of the largest quantitative targeted proteomics data sets in mammalian tissues. Our results revealed rapid response to high-fat diet that diverged early in the feeding regimen, and evidenced a response to high-fat diet dominated by the activation of peroxisomal β-oxidation in C57BL/6J and by lipogenesis in 129Sv mice.
Molecular Systems Biology 9: 681; published online 16 July 2013; doi:10.1038/msb.2013.36
Subject Categories: proteomics; molecular biology of disease
Keywords: liver; metabolic syndrome; NAFLD; proteomics; SRM

Introduction

The metabolic syndrome is a combination of medical disorders—including central obesity, insulin resistance, dyslipidemia, hypertension and hepatic steatosis—and predisposes to a range of diseases such as diabetes, cardiovascular disease and cancer (Eckel *et al*, 2010). Genetic and environmental components contribute to the initiation and establishment of this disorder, but it remains unclear how these factors interact to produce the metabolic syndrome and its related pathologies (Biddinger *et al*, 2005). A deregulation of the hepatic lipid metabolism has been proposed as one of the major features in the pathogenesis of the metabolic syndrome (Luyckx *et al*, 2000; Marchesini *et al*, 2001; Pagano *et al*, 2002). This disorder, which is also known as non-alcoholic fatty liver disease (NAFLD), leads to an increased storage of triacylglycerides in the liver and has been strongly associated with selective hepatic insulin resistance, i.e., the failure of insulin to suppress gluconeogenesis while sustaining the activation of lipolysis (Dixon *et al*, 2001, 2004).

In spite of intense research, the complex etiology of insulin resistance and its association with the accumulation of triacylglycerides in liver is not yet completely understood. Several studies have recently used mice of different genetic backgrounds as a model to study the link between insulin-regulated networks and hepatic steatosis, and thus to identify potential genetic elements controlling the progression of the metabolic syndrome and its associated pathologies. In this regard, the effect of genetic heterogeneity on the development of diabetes was recently evaluated using genetically engineered variants of the mouse strains C57BL/6J (B6) and 129Sv (S9). Double heterozygous knockout mutations of the insulin receptor (IR) and insulin receptor substrate-1 (IRS-1) genes were generated on both backgrounds and the mice were tested for insulin resistance after a high-fat diet regimen (Kulkarni *et al*, 2003). The data showed that the phenotypes of these strains differed dramatically. The C57BL/6J double heterozygous mice showed marked hyperinsulinemia and islet hyperplasia and they developed early hyperglycemia and diabetes. In contrast, the 129Sv double heterozygous mice showed mild hyperinsulinemia, minimal islet hyperplasia and

they hardly developed diabetes. Biddinger *et al* (2005) also reported acute phenotypic differences after several weeks of high-fat diet in wild-type C57BL/6J and 129Sv mice. Wild-type C57BL/6J and 129Sv mice were fed, in that case, with either a low-fat or high-fat diet to dissect the interaction of diet and genetic background under normal conditions. After several weeks of high-fat diet, the 129Sv mice developed typical features of the metabolic syndrome, such as obesity, hyper-insulinemia and glucose intolerance. In contrast, the C57BL/6J mice developed these features on both diets. In both strains, high-fat feeding led to increased hepatic steatosis and it decreased serum triglyceride levels and hypercholesterolemia, although the C57BL/6J mice developed a more serious steatosis and a larger increase in low-density lipoprotein (LDL) cholesterol than the 129Sv mice (Biddinger *et al*, 2005). Therefore, under constant conditions, these genetically different mouse strains show markedly different metabolic phenotypes.

Several proteomics studies have analyzed different mouse strains in the past to relate observed phenotypes to protein changes in the context of the metabolic syndrome (Park *et al*, 2004; Schmid *et al*, 2004; Kirpich *et al*, 2011). However, most of these studies covered only a few experimental conditions and did not address the dynamics of the biological system at different time points, different treatments and in different mouse strains. The number of experimental conditions to be meaningfully compared in proteomics studies has traditionally been limited by the sampling effect of the frequently used discovery proteomic technique (Domon and Aebersold, 2010), which increases the number of missing values and thus, the sparseness of the data matrix (Bensimon *et al*, 2012) with increasing number of samples analyzed. Targeted proteomics by selected reaction monitoring (SRM) overcomes these technical limitations and constitutes the method of choice for the consistent quantification of a limited number of predefined proteins in multiple samples and conditions (Picotti *et al*, 2009; Costenoble *et al*, 2011; Sabido *et al*, 2012).

In the present study, we used targeted mass spectrometry by SRM to generate accurate quantitative measurements in mouse liver homogenates, of proteins involved in the insulin-signaling pathway and central metabolism across 12 different conditions, with 3 biological replicates each. A total of 144 proteins—including metabolic enzymes, kinases, phosphatases, transcription factors and structural proteins—were reproducibly quantified in all samples representing different treatments, time points and mouse strains, thus generating a rich and near complete quantitative proteomics data set to evaluate the differential changes induced in the proteome after subjecting C57BL/6J and 129Sv mice to a sustained long-term high-fat diet. The data set revealed a rapid proteomic response to high-fat diet that diverged early in the feeding regimen in the obesity prone C57BL/6J mouse strain and the partially obesity and diabetes-resistant 129Sv strain.

Results

SRM assay development for targeted proteomics

SRM assays were initially designed to quantify 257 proteins covering the insulin-signaling pathway and the lipid and carbohydrate metabolism pathways (Figure 1; Supplementary Table S1). SRM assays corresponding to 2–4 unique peptides per protein were developed, using synthetic peptides and following the general high-throughput strategy previously reported (Picotti *et al*, 2010). The peptides were selected based on the number of observations in previous MS experiments (Martens *et al*, 2005; Desiere *et al*, 2006) or, when no previous evidence was available, on the MS-suitability score predicted by PeptideSieve (Mallick *et al*, 2007). Out of the data generated from these peptides a spectral library containing SRM assays for 1418 peptides representing the 257 proteins was generated. These assays were used throughout this study to quantify the targeted proteins under different conditions and treatments to study the effect of high-fat diet on insulin-regulated signaling networks and hepatic steatosis, and they are all available in Supplementary information (Supplementary Table S1).

Mouse strains C57BL/6J and 129Sv were selected for this study as they show distinctive phenotypic differences in response to a sustained high-fat diet. Indeed, after several weeks of high-fat diet the C57BL/6J mice showed higher lipid accumulation in the liver, higher weight increase, a pronounced hyperglycemia and higher hyperinsulinemia when compared with the 129Sv strain (Supplementary Table S2).

Liver samples from mice fed with a high-fat rodent diet for 0, 6 and 12 weeks were homogenized, and the lysate of a SILAC (stable incorporation of labeled amino acids in cell culture) labeled mouse hepatocyte cell line was spiked in as an internal heavy-labeled reference. Whole cell homogenates were digested and subsequently fractionated by off-gel electrophoresis, and equal amounts of total protein were analyzed with targeted nLC-SRM. All experiments were done in triplicate. A total of 251 peptides representing 144 of the preselected proteins involved in the insulin-signaling pathway and central metabolism (Figure 1; Supplementary Table S3A) were consistently detected and quantified across different treatments (fasted overnight and fed *ad libitum*), strains and time points using targeted mass spectrometry. Proteins that could not be detected even after sample fractionation mostly corresponded to transcription factors and signaling proteins, which are normally present in the cell only at low abundance levels. Acquired data are summarized in Figure 2 and Supplementary Table S3.

Unsupervised hierarchical clustering of all protein abundance changes showed two clearly distinct groups corresponding to the studied mouse strains, thus confirming the importance of the genetic background as the main determinant modulating the response to high caloric intake. The subset of identified proteins that more strongly contributed to the separation of the mouse strains were mainly metabolic enzymes belonging to the tricarboxylic acid cycle, glycolysis, β-oxidation, fatty acid biosynthesis and glycogen metabolism (Figure 2A; Supplementary Table S4A). Similar results were obtained when the data were subjected to a principal component (PC) analysis, although, in that case, also proteins distinguishing different time points and treatments could be identified (Figure 2B; Supplementary Table S4B). Three PCs were required to distinguish among strains, time points and treatments showing that there is enough variation in the abundance of the measured peptides and proteins to reflect the different conditions of the study (PC-1: 64.0%; PC-2:
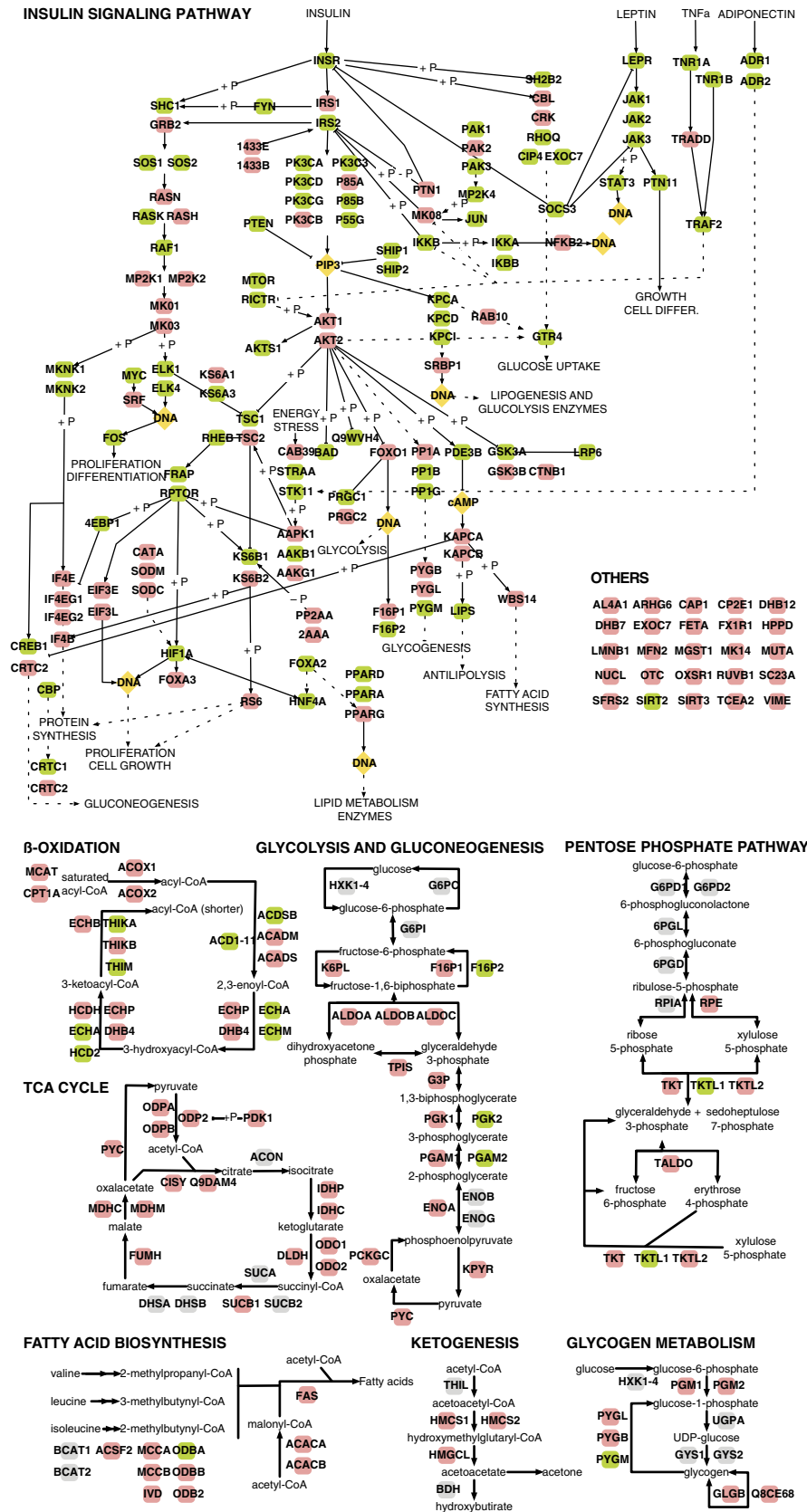
Figure 1 Schematic representation of the insulin-signaling and the central metabolic pathways. SRM assays were developed for the proteins colored in red and green. Gray-colored proteins indicate proteins not targeted in the study. Red colors indicate proteins that were consistently detected and quantified in murine liver. Yellow diamonds represent either DNA or small molecules. Protein codes refer to the Uniprot database identifiers without the suffix _MOUSE.

A

B
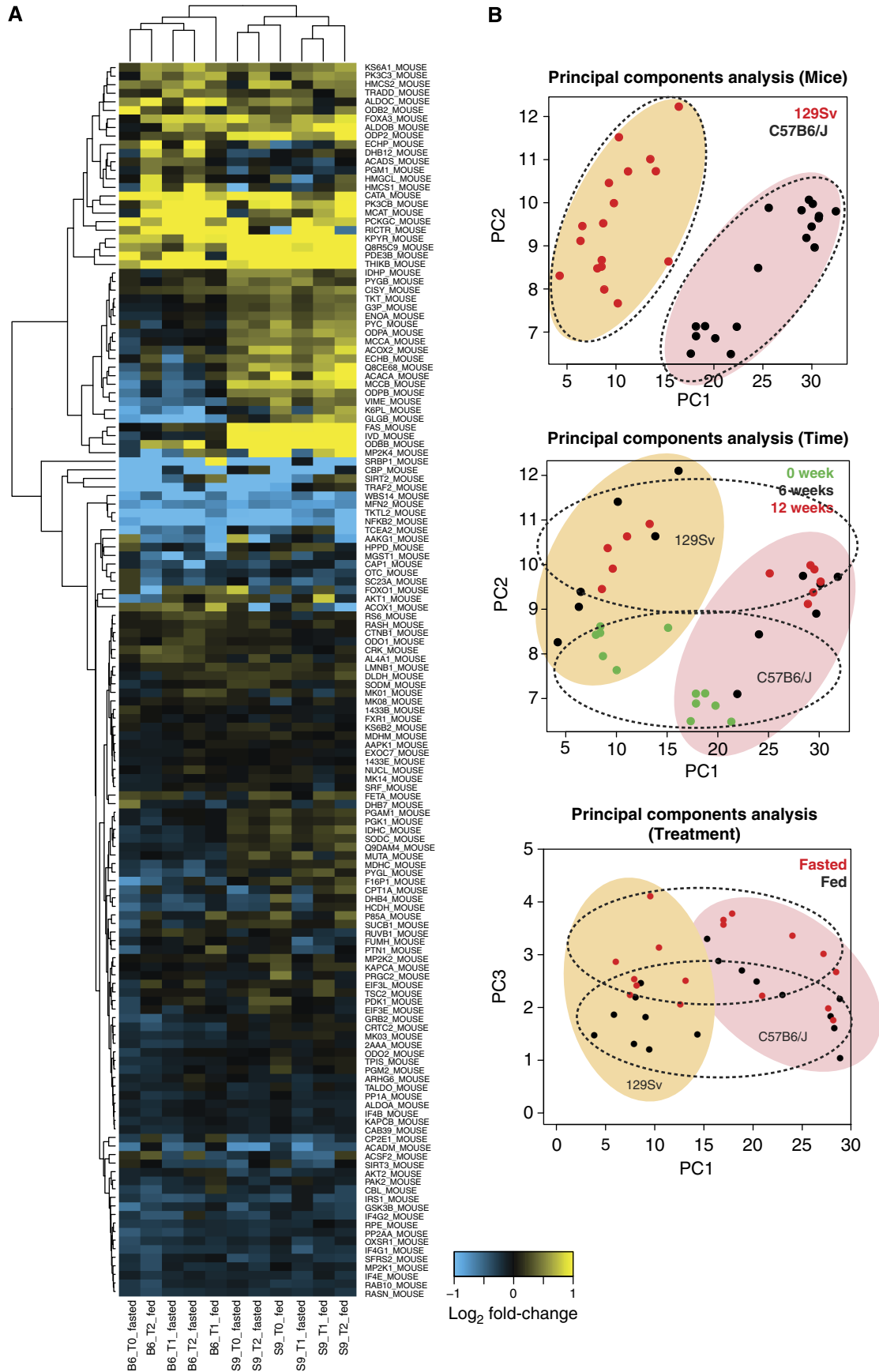
10.4%; PC-3: 5.7% of the total variation). Each PC was orthogonal to the previous ones, and uncovered complementary variation. Together, the three components explained over 80% of the total variation (Figure 2B, dashed ellipses). These analyses showed that although the observed variation is mostly due to differences among mouse strains, time points and treatments still have a significant contribution to sample variability. These observations confirmed the rich information content of the acquired data and provided us with a first overview of the system under study. Further, detailed evaluation of the observed differences in the targeted proteome among mouse strains, time points and treatments is described in the next sections.

Comparison of mouse strains to elucidate the differential effect of the high-fat diet

The quantitative data set acquired for the targeted proteins was initially used to evaluate the changes in protein abundance within each mouse strain after 6 and 12 weeks of high-fat diet under *ad libitum* condition. In both strains, several proteins exhibited significant changes in abundance after 6 (T1) and 12 weeks (T2) of high-fat diet. Most of the observed changes were found in proteins involved in the β-oxidation (DHB4 in C57BL/6J) and fatty acid biosynthetic pathways, as well as in proteins involved in glucose metabolism (Figure 3A and B; Supplementary Table S5). Moreover, some proteins involved in the insulin-signaling pathway, such as transcription factors SRBP1 and EIF3L and kinase MK01, showed significant abundance changes by mass spectrometry either in one (EIF3L in C57BL/6J) or both mouse strains (MK01 and SRBP1) (Figure 3B; Supplementary Figure S2). Overall, the fed C57BL/6J mice showed a more significantly altered targeted proteome after several weeks of high-fat diet than the fed 129Sv mice.

The detected time-dependent changes in expression levels may, however, reflect diet-induced alterations as well as age-dependent changes. Therefore, to elucidate the differential effect of a sustained high-fat diet in the proteome of C57BL/6J and 129Sv mice, we directly compared protein abundances in the two mouse strains at the same points of the regimen. This analysis revealed numerous proteins that showed different quantitative trajectories after several weeks of high-fat diet in the two strains. The data in Figure 4A, Supplementary Figure S3 and Supplementary Table S6 show that this differential response affected proteins in the main metabolic pathways, especially fatty acid synthesis and β-oxidation, and in the insulin-signaling pathway. The proteins involved in the insulin-signaling pathway that show strain-dependent responses to high-fat diet include several kinases such as KAPCA, KAPCB, GSK3B, PK3C3, PDK1, MP2K4, MK01, the oxidative stress enzymes CATA, SODM, and the transcription factor SRBP1 (Figure 4D).

Among proteins with different fold changes in the two mouse strains after either 6 or 12 weeks treatment, we observed numerous proteins that showed opposite quantitative trends in response to high-fat diet (Figure 4A and C). This was the case of several enzymes related to the TCA cycle (ODP2, ODPA, ODPB, CISY) and of some key proteins involved in the lipid biosynthetic pathway such as FAS and Q8R5C9 (ACACB), which showed increasing abundance levels in C57BL/6J whereas protein abundance was decreased in 129Sv mice. Other proteins that also exhibited opposite quantitative trends were some β-oxidation-related proteins (ACOX1 and ECHB), and pyruvate kinase (KPYR), a key enzyme in glycolysis (Figure 4A and D). Most of these proteins coincide with the proteins identified in the initial unsupervised hierarchical clustering as the subset of proteins most strongly differentiating the mouse strains.

Among the proteins showing opposite quantitative patterns over time in the two mouse strains were not only proteins related to central metabolism but also other regulatory proteins such as the insulin-related cAMP-dependent protein kinase (KAPCA) (Figure 4D). The abundance of the former protein is significantly increased at the 12-week time point in C57BL/6J mice. This pattern is consistent with the inhibition of fatty acid synthesis and the promotion of the transcription of genes encoding lipid catabolic enzymes. Temporal behavior in protein abundance also differed between strains for SRBP1, a transcription factor that exhibits highly increased levels in 129Sv mice and that activates the transcription of genes related to hepatic lipogenesis (Figure 4A, golden squares; Supplementary Table S6). The observed differences in the abundance of these regulatory proteins between strains suggest that peroxisomal β-oxidation is actively promoted in fatty C57BL/6J mice after several weeks of high-fat diet, whereas lipogenesis activation dominates the response of 129Sv mice under the same conditions.

Other proteins with significant differences in protein abundance between strains showed the same direction but different magnitude in response to high-fat diet. This is the case for proteins related to glycolysis and gluconeogenesis, for enzymes involved in ketogenesis and glycogen synthesis, and for several kinases and signaling proteins (Figure 4A, gray squares; Supplementary Table S6).

Most proteins with a differential temporal response to high-fat diet between the strains targeted in this study already showed this differential response within the first 6 weeks of high-fat diet (Figure 4B, red and blue dots), and in many cases differences persisted in the 6- to 12-week period (Figure 4B, red dots). Only few proteins showed a delayed response when comparing strains, i.e., they exhibited a significantly different abundance only in the 6- to 12-week period of high-fat diet. Among these are proteins related to oxidative stress (CATA and SODM)—a process that has recently been linked to the metabolic syndrome (Roberts and Sindhu, 2009; Whaley-Connell *et al*, 2011)—some β-oxidation and fatty acid

Figure 2 (**A**) Heatmap and unsupervised hierarchical clustering of protein abundance fold-changes of all samples with respect to the reference sample C57BL/6J (B6) mice fed *ad libitum* at 0 week (T0). T1 refers to animals after 6 weeks of high-fat diet and T2 corresponds to 12 weeks of high-fat diet. S9 is the abbreviation for 129Sv mice. (**B**) Principal component analysis of the relative protein abundance measured in different mouse strains, different time points after a sustained high-fat diet and different treatments. Three different principal components are required to distinguish between strains, time points and treatments. Orthogonality between the principal components is highlighted by dashed ellipses (PC-1: 64.0%; PC-2 10.4%; PC-3 5.7% of the total variation).
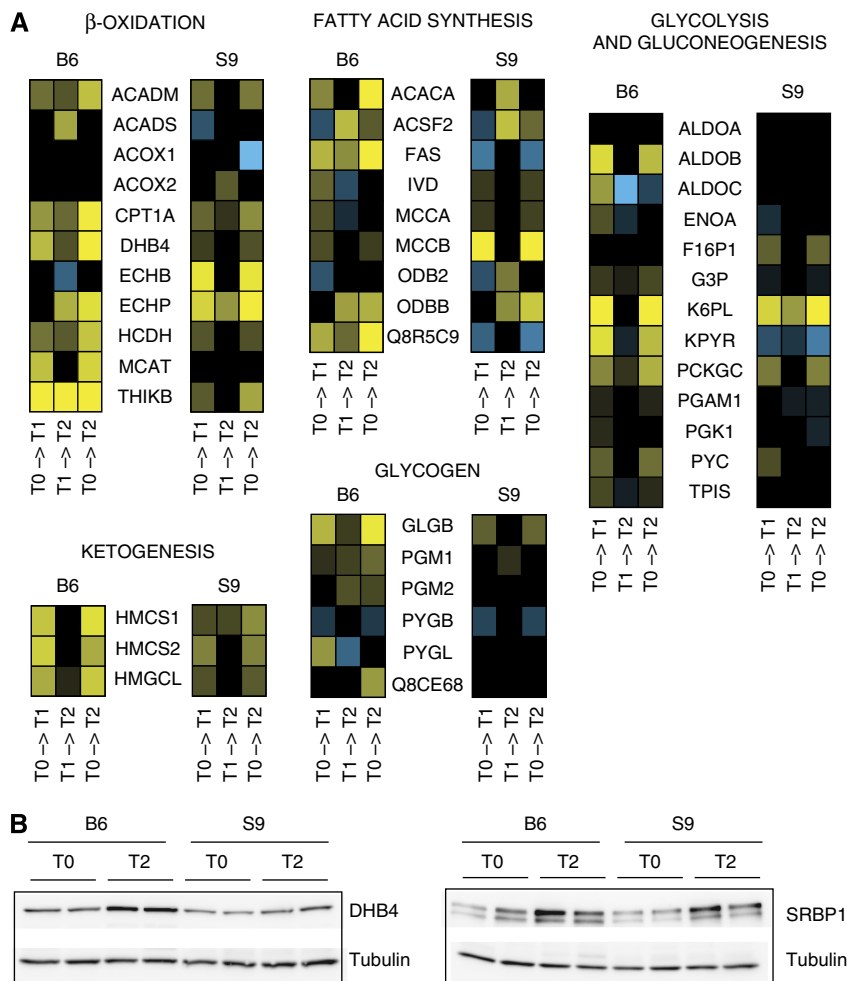
Figure 3 (**A**) Changes in protein abundance after 6 (T1) and 12 weeks (T2) of high-fat diet in C57BL/6J (B6) and 129Sv (S9) mice fed *ad libitum*. Colors represent either increased (yellow) or decreased (blue) protein abundances, while the color intensity reflects the corresponding log$_2$(fold change). Proteins were grouped according to metabolic pathways. Proteins with no significant fold-change are presented in black. All experiments were done in triplicate. Protein codes refer to the Uniprot database identifiers without the suffix _MOUSE. (**B**) Protein abundance of DHB4 and SRBP1 after 6 (T1) and 12 weeks (T2) of high-fat diet in C57BL/6J (B6) and 129Sv (S9) mice fed *ad libitum* validated by western blot.

metabolism enzymes (ACADM, HCDH and MCCA), as well as other proteins related to the insulin-signaling and other pathways (SRF, RICTR, EIF3L, PGM2, OTC, VIME and DHB12) (Figure 4B, green dots). Overall, most of the strain-specific changes therefore were apparent early in the regimen when phenotypic changes were already set, but not yet very pronounced.

Influence of high-fat diet in the fed–fasting transition

We were also interested in establishing the effects of a persistent high-fat diet on the proteome changes observed in the fed–fasting transition. To address this question, we first analyzed those changes that take place in the normal proteome in the fed–fasting transition (i.e., in the initial time point: T0 or 0 weeks) and compared them between strains. Then, we asked whether the proteins initially showing a similar abundance profile between strains were perturbed after 12 weeks of high-

fat diet and whether the potential perturbations were strain specific.

The analysis of the fed–fasted transition at the initial time point showed that several enzymes involved in β-oxidation and gluconeogenesis reacted similarly to fasting in both mouse strains (Figure 5A, both panels; Supplementary Tables S7 and S8), whereas numerous proteins involved in glycolysis, gluconeogenesis and fatty acid synthesis already showed a different pattern at the initial time point (Figure 5B; Supplementary Table S9). These differences, which were already present before any diet treatment, mostly reflect the different genetic backgrounds of both mouse strains.

Several proteins that showed no abundance differences between strains in the initial response to the fed–fasting transition had a differential response to fasting after 12 weeks of high-fat diet. The identification of these proteins is of special interest to ascertain the differential effects of high-fat diet on the fed–fasting transition in each mouse strain and, thus, to identify potential alterations in response to food intake
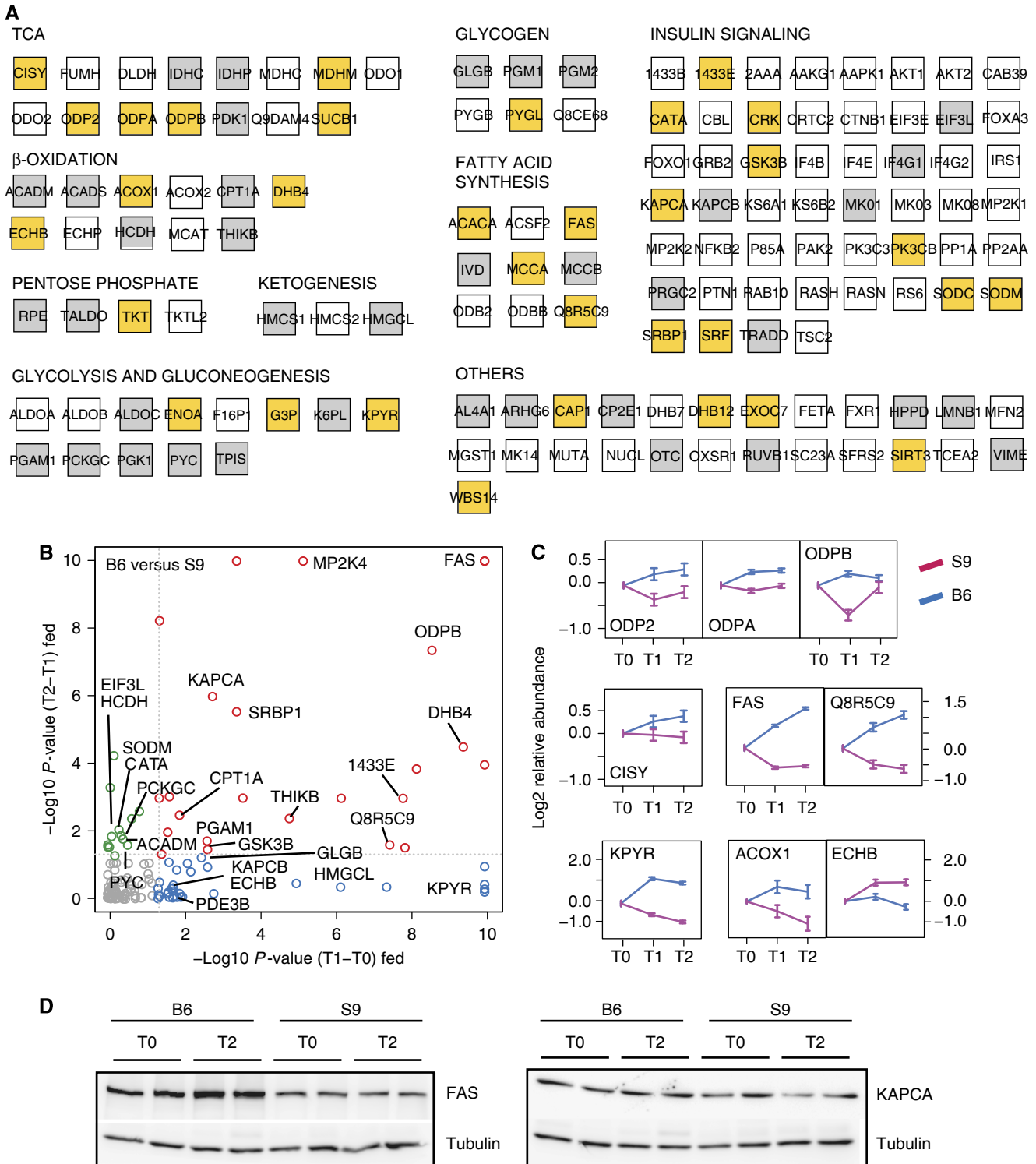
A

Figure 4 (**A**) Quantified proteins grouped by metabolic or signaling pathway. Highlighted proteins (both in gray and gold) correspond to proteins showing a different profile when comparing the mouse strains fed *ad libitum* at different time points. Gray-colored features correspond to proteins with a significant change between strains but showing a similar trend, i.e., showing an increase (or decrease) in protein abundance over time in both strains. Gold-colored features indicate proteins showing opposite trends in the fold-change. (**B**) Scatter plot of *P*-values obtained when comparing protein abundance changes between mouse strains at the early stage of high-fat diet—i.e., from 0 (T0) to 6 (T1) weeks (x axis)—and at its late stage—from 6 (T1) to 12 (T2) weeks (y axis). The plot is divided into three main parts: (i) proteins with a different profile between strains at the early stage (blue dots); (ii) proteins with a different profile between strains only at the late stage (green dots); and (iii) proteins with a different profile between strains at both the early and late stages (red dots). (**C**) Relative abundance profiles of selected proteins at 0 (T0), 6 (T1) and 12 (T2) weeks of high-fat diet for each mouse strain (B6, blue; S9, pink) fed *ad libitum*. Error bars correspond to standard errors. (**D**) Protein abundance of FAS and KAPCA after 6 (T1) and 12 weeks (T2) of high-fat diet in C57BL/6J (B6) and 129Sv (S9) mice fed *ad libitum* validated by western blot.
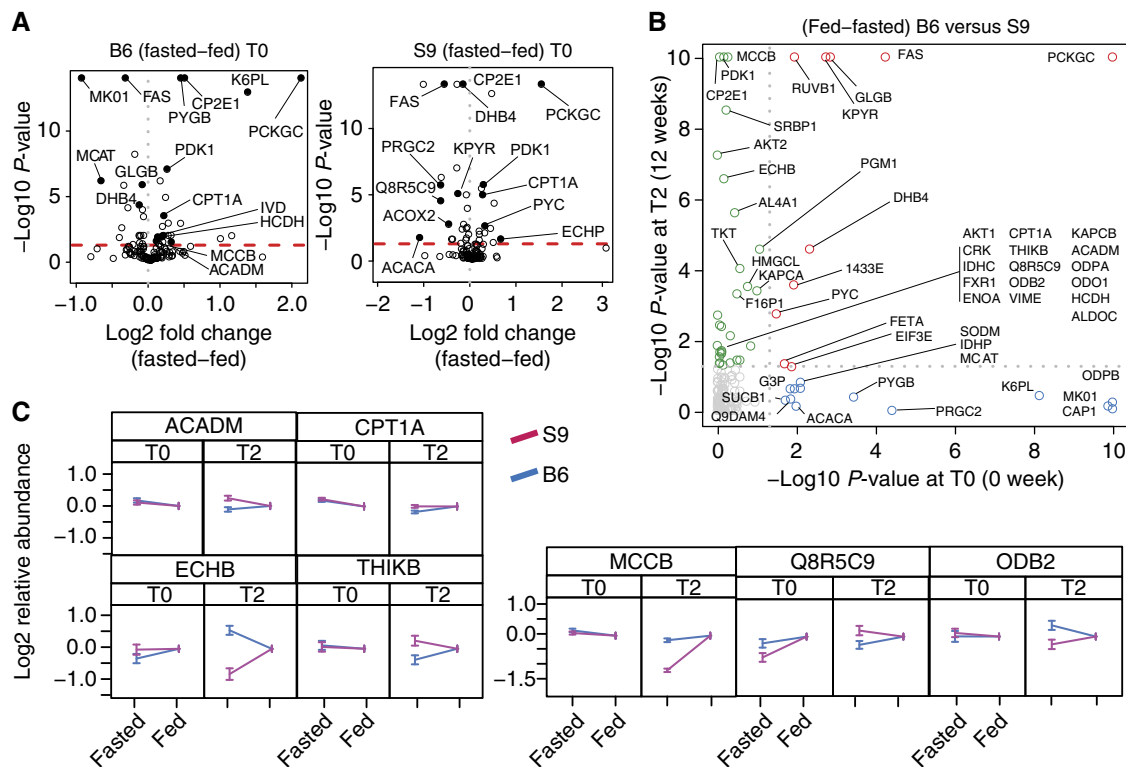
Figure 5 (**A**) Observed significant protein fold-changes during the fed–fasting transition in C57BL/6J (B6) and 129Sv (S9) mice fed with a normal diet (T0). Significance threshold was set at adjusted *P*-value of 0.05. (**B**) Scatter plot of *P*-values associated with the observed changes when comparing both mouse strains fed in normal diet—i.e., 0 weeks (T0, x axis); and after 12 weeks of high-fat diet (T2, y axis). The plot is divided into three main parts: (i) proteins with a different fasting-response pattern at normal diet (blue dots); (ii) proteins with a different fasting response among strains only after 12 weeks of high-fat diet (green dots); and (iii) proteins with a different fasting response both in normal diet and after 12 weeks of high-fat diet (red dots). (**C**) Protein abundance changes in the fed–fasting transition of selected proteins at 0 (T0) and 12 (T2) weeks of high-fat diet for each mouse strain (B6, blue; S9, pink). Error bars correspond to standard errors.

(Figure 5B, green dots; Supplementary Tables S9 and S10). Among these proteins was the SRBP1 transcription factor that is involved in the regulation of lipogenesis, numerous proteins involved in lipid metabolism (ACADM, ECHB, THIKB, CPT1A, MCCB, ODB2 and Q8R5C9), and several kinases that regulate the cellular response to insulin (AKT1, AKT2, KAPCA, KAPCB and PDK1). Together, these results indicate that a high-fat diet has a major impact on the proteome regulating lipid metabolism and, most probably, also on the phosphoproteome that mediates the signaling cascade in response to fasting or food intake (Figure 5C). Finally, some of the proteins that had a different initial (T0) response to fasting when comparing both strains also showed a different behavior after being subjected to a high-fat diet. This is the case of FAS, PCKGC, GLGB, KPYR, PYC and DHB4, among others (Figure 5B, red dots; Supplementary Figure S4).

Discussion

The experimental design of quantitative proteomic studies to date has been limited to a low number of different experimental conditions (e.g., wild-type versus mutant strains). Three main reasons have precluded the systematic comparisons of larger numbers of sample proteomes. The first is the under sampling effects of the prevalent discovery proteomics techniques that results in the irreproducible detection and quantification of proteins, particularly in complex samples. The effect is compounded by the observation that lower abundance proteins show a lower degree of reproducibility than more highly expressed proteins (Domon and Aebersold, 2006; Michalski *et al*, 2011). The second reason is the limited number of labeling plexes that are available in the available isotopic or isobaric labeling protocols (Dephoure and Gygi, 2012) and third, is the limited dynamic range of label-free LC-MS pattern comparison methods which are inherently scalable but lack the analytical depth to quantify low abundance proteins. From a systems biology point of view, where a main objective is the quantitative measurement of a specific biological system under differentially perturbed states (Ideker *et al*, 2001; Bensimon *et al*, 2012) the comparative analysis of a larger number of samples and replicates is highly desirable. Targeted proteomics by SRM overcomes many of the aforementioned limitations and permits the consistent quantification of a pre-defined set of proteins in multiple samples and conditions.

In the present study, we developed a set of SRM assays to systematically quantify murine proteins involved in the insulin-signaling pathway and central metabolism in an experimental design that intends to assess the changes of this system during the emergence of metabolic syndrome. The metabolic syndrome is a combination of medical disorders,

including central obesity, insulin resistance, dyslipidemia, hypertension and hepatic steatosis. These disorders predispose the patient to several diseases such as diabetes, cardiovascular disease and cancer, and in the last years this syndrome has become an important problem for the national health-care systems of most western countries. In spite of significant efforts by the scientific community and the extensive knowledge that has accumulated about individual enzymes and regulatory proteins, the complex etiology of insulin resistance and its association with the accumulation of lipids in liver is not yet completely understood. To obtain, for the first time, a comprehensive quantitative overview of the behavior of some of the main pathways involved in metabolic syndrome at the protein level, we designed a study in which the effect of three variables, genetic background, time and fed/fast state on the system was systematically tested. Over 200 mouse proteins involved in the insulin-signaling pathway and the central metabolism were initially selected for quantitative targeted analysis. SRM assays were developed for each of the selected proteins and used to assess their detectability at endogenous levels. The developed SRM assays will be publicly available and provide a resource for others researchers to easily quantify the selected proteins in other studies. The targeted proteomic measurements were finally performed for 144 proteins across 36 samples, thus generating a protein abundance versus condition matrix of 5184 quantitative data points with a high degree of completion. The 36 conditions consisted of triplicates of liver samples from two genetically different mouse strains (C57BL/6J and 129Sv) each measured at three time points at fed and fasted state, thus becoming one of the biggest targeted proteomics studies performed in mammalian tissues.

These two mouse strains were selected due to their different response to a sustained high-fat diet under normal conditions. Wild-type C57BL/6J mice showed altered physiological parameters such as higher body weight, increased fat accumulation in the liver, hyperglycemia and hyperinsulinemia, whereas 129Sv mice show an increased resistance to these phenotypic alterations.

Despite the size of the data set and the consistency among measurements, our approach also had some limitations as not all the initially selected proteins could be finally quantified in the endogenous sample. Undetected targeted peptides mostly come from proteins present in low concentrations in the sample, peptides with low response to mass spectrometric analysis or peptides with high interfering signals. Nevertheless, detected proteins spread over all the different branches of the insulin-signaling pathway and covered most of the targeted central metabolism proteins, thus providing us with a complete overview of the current response of these pathways to a sustained high-fat diet.

Initially, we evaluated proteins that showed different abundance profiles after several weeks of high-fat diet when directly comparing C57BL/6J and 129Sv mouse strains. Most of the observed changes were already evident within the first 6 weeks of high-fat diet, and they mainly targeted β-oxidation, fatty acid biosynthetic pathway and the insulin-signaling pathway. Significant protein abundance changes were detected in essential kinases such as KAPCA, KAPCB, GSK3B, PK3C3, PDK1, MP2K4 and MK01, which modulate

intracellular responses to glucose uptake and insulin stimulation and determine downstream phosphorylation patterns. These results point to potential changes in the liver protein phosphorylation status induced by long-term high-fat diet; and therefore, follow-up phosphoproteome studies might be relevant in this context.

Overall, the observed differences suggest that peroxisomal β-oxidation is activated in fatty C57BL/6J mice after several weeks of high-fat diet whereas lipogenesis dominates the response of 129Sv mice under the same conditions. For instance, the different protein abundance profiles of insulin-related cAMP-dependent protein kinase (KAPCA) and the sterol regulatory element-binding protein 1 (SRBP1) observed in 129Sv and C57BL/6J mice suggest an increased activity of peroxisomal β-oxidation in fatty C57BL/6J and a lipogenesis activation in 129Sv mice under the same conditions. This observation might be related to strain differences in AMP-activated protein kinase (AMPK) activation after a sustained high-fat diet. AMPK has previously been described as a molecular switch, associated with metabolic disorders, that modulates the activity of catabolic and anabolic pathways based on the energetic needs (Cantó *et al*, 2009).

Moreover, when evaluating the differential effect of a sustained high-fat diet in C57BL/6J and 129Sv mice, our results suggest that these strains exhibit a rapid and differential response to high-fat diet affecting most of the targeted proteins. These results indicate therefore that 6 weeks (T1) of treatment are sufficient to substantially change the landscape of the liver proteome related to insulin signaling and central metabolism. This observation is consistent with the previously reported physiological differences between these two mouse strains (Almind and Kahn, 2004). The changes detected in the proteome are, however, more rapid since they allow a clear discrimination of phenotypes at a much earlier stage than in other long-term experiments in which the high-fat diet expanded over 18 weeks (Biddinger *et al*, 2005).

Finally, we found that a persistent high-fat diet does not only differentially affect abundance of proteins participating in the main metabolic pathways and signaling pathways, but it also alters the transient changes that normally occur in C57BL/6J and 129Sv mice when individuals shift from a fed to a fasted state. In this regard, our results indicate that high-fat diet leads to major protein abundance changes in the cellular response to fasting or food intake even if acknowledging that some of the changes observed between strains can be ascribed to the different genetic backgrounds of the two mouse strains (Kulkarni *et al*, 2003).

In conclusion, the study here reported constitutes one of the largest quantitative and dynamic targeted proteomics studies performed in mammalian tissues. The large data set generated has allowed us to study the effects of diet, genetic background and fasting in the context of the metabolic syndrome. Our analyses detected a rapid and different response in the two mouse strains to a sustained high-fat diet. Indeed, the response in the C57BL/6J mice is mainly characterized by the activation of peroxisomal β-oxidation, whereas lipogenesis likely dominates the response of the diabetes-resistant 129Sv mice. Our systemic proteomics approach to study the metabolic syndrome in mice can not only contribute to a better understanding of this syndrome in humans but it has proven

that proteomics can generate the consistent protein versus condition data sets required to analyze the dynamics of biological systems.

Materials and methods

Animals

Three-week-old C57BL/6J and 129Sv mice were obtained from Charles River Laboratories International, Inc. The mice were maintained in chow diet for 1 additional week before starting the experiments with high-fat diet in a pathogen-free facility at the Institute of Molecular Systems Biology, ETH Zürich, complying with official ETH Zürich ethical guidelines. Mice from both strains were kept on a 12-h light/dark cycle and fed with a high-fat rodent diet (60% fat content) once the experiments were started.

C57BL/6J and 129Sv mice were fed *ad libitum* with a high-fat rodent diet for 0, 6 and 12 weeks according to the experimental design. In addition to the time and strain genotype, a third factor (treatment) was included in the experiment, whereby two groups were defined. The first group contained mice fasted overnight before they were killed. Mice of the second group were fed *ad libitum*. Fasted condition was controlled by serum biochemical parameters and the abundance of transcription factor SRBP1 known to be significantly decreased after a fasting period (Supplementary Table S2; Supplementary Figure S5). Therefore, the overall experimental design consisted of 12 different conditions (3 time points, 2 mouse strains and 2 treatments) with $n = 3$ animals in each group.

Sample preparation

PBS-perfused mouse livers were homogenized using RIPA-modified buffer (1% NP-40, 0.1% sodium deoxycholate, 150 mM NaCl, 1 mM EDTA, 50 mM Tris pH 7.5, protease inhibitors EDTA-free, 10 mM NaF, 10 mM sodium pyrophosphate, 5 mM 2-glycerophosphate) and a glass-glass tight douncer homogenizer (Wheaton Science Products, USA). Homogenates were centrifuged (20 000 g, 4°C, 15 min) and the supernatant was collected and kept at 4°C. Pellets were resuspended with Urea-Tris buffer (50 mM Tris pH 8.1, 75 mM NaCl, 8 M urea, EDTA-free protease inhibitors, 10 mM NaF, 10 mM sodium pyrophosphate, 5 mM 2-glycerophosphate), and after sonication, they were centrifuged again (20 000 g, 4°C, 15 min). The new supernatant was collected and mixed with the previous one. The resulting pellets were discarded. The total protein content was quantified with the BCA Protein Assay (Thermo Fisher Scientific, USA) using bovine serum albumin as a standard. Aliquots of the homogenates were immediately prepared and stored at −80°C. Sample quality and concentration were also assessed with SDS–PAGE and silver staining (Supplementary Figure S1).

In all, 1 mg of total protein was mixed with 1 mg of the heavy isotope-labeled reference proteome (see below for details) and the combined sample was precipitated overnight with six volumes of ice-cold acetone (16 h, −20°C) for mass spectrometric analysis. The supernatant was discarded and the pellets were dried and resuspended in freshly prepared digestion buffer (8 M urea, 0.1 M NH$_4$HCO$_3$). Samples were reduced with 12 mM dithiothreitol (30 min, 37°C) and alkylated with 40 mM iodoacetamide (45 min, 25°C) in the dark. Samples were diluted with 0.1 M NH$_4$HCO$_3$ to a final concentration of 1.5 M urea and digested overnight at 37°C with sequence grade trypsin (10 µg, Promega AG, Switzerland). After digestion, peptide mixtures were acidified to pH 2.8 with TFA and desalted with 500 mg Sep-Pak tC$_{18}$ silica cartridges (Waters Inc., USA). Samples were dried under vacuum before off-gel fractionation (24 wells, 3–10 pI strips) in a 3100 OFFGEL Fractionator (Agilent Technologies). Peptide mixtures collected in each well were pooled in six different fractions (A: wells 1 and 2, B: wells 3 and 4, C: wells 5–8, D: wells 9–11, E: wells 12–18 and F: wells 19–24), acidified to pH 2.8 with trifluoroacetic acid and desalted with MacroSpin C18 silica columns (The Nest Group Inc., USA). Samples were dried under vacuum and re-solubilized to 1 µg µl^{-1} in 0.1% formic acid and 2% acetonitrile before mass spectrometric analysis.

Preparation of the heavy-labeled reference proteome

A Hepa1-6 mouse cell line was obtained from the American Tissue Type Culture Collection (cat. CRL-1830), labeled with SILAC medium and used as a heavy-labeled reference proteome in all samples. Cells were grown at 37°C and 5% CO$_2$ in L-lysine- and L-arginine-depleted DMEM high glucose medium (Caisson Laboratories Inc.) supplemented with 10% dialyzed FCS (BioConcept), 1% penicillin/streptomycin (Invitrogen) and L-^{13}C$_6$^{15}N$_4$-arginine and L-^{13}C$_6$^{15}N$_2$-lysine (Sigma-Aldrich GmbH). Cells were cultured in 150-cm^2 plates and passaged at 80% confluence. The incorporation of the heavy amino acids was regularly checked by mass spectrometry on cell aliquots and the culture was maintained until an incorporation of heavy amino acids >95% was achieved. Cells were then washed with ice-cold PBS, scraped from the plates and homogenized as described above.

Target protein selection

In all, 257 proteins involved in the insulin-signaling pathway and in the lipid and carbohydrate metabolism pathways were selected for quantification using targeted mass spectrometric analysis. This set of proteins includes almost all the enzymes involved in β-oxidation, fatty acid synthesis, ketogenesis, glycogen synthesis and degradation, pentose phosphate pathway, glycolysis, gluconeogenesis and TCA cycle. Moreover, proteins of the different branches of the insulin-signaling pathway, as well as downstream effectors, and a few other proteins potentially linked to the metabolic syndrome, were also included in the final set of targeted proteins. Together, the selected set of proteins covered several protein classes (e.g., metabolic enzymes, kinases, phosphatases and transcription factors), and spanned a large dynamic range of cellular abundance, ranging from the few thousands of copies per cell (c.p.c.) of the nuclear factor NF-kappa-β (4000 c.p.c.) to the more than hundred thousand copies per cell in the case of fatty acid synthase (>140 000) (Schwanhäusser *et al*, 2011). The proteins selected for targeting are listed in Supplementary Table ST1A.

SRM assay development

SRM assays were developed following the general high-throughput strategy previously reported (Picotti *et al*, 2010). Initially, 4–6 unique peptides ranging from 6 to 20 amino acids in length, containing tryptic ends and no miscleavages, were chosen for each of the selected proteins. Unique peptides previously observed in discovery MS experiments (Martens *et al*, 2005; Desiere *et al*, 2006) were prioritized during the peptide selection process. For those proteins for which no peptides had been reported previously (i.e., for previously unidentified proteins), peptide selection was based on the MS-suitability score computed by PeptideSieve (Mallick *et al*, 2007). All peptides containing amino acids prone to undergo unspecific reactions (e.g., Met, Trp, Asn and Gln) were generally avoided and only selected when no other options were available (Lange *et al*, 2008). The selected peptides were chemically synthesized via SPOT synthesis (JPT Peptide Technologies) and used in unpurified form for the SRM assay development. Fragment ion spectra were collected for each peptide using SRM-triggered MS^2 mode and two predicted high mass y-ions per peptide in a QTRAP 4000 instrument (AB/Sciex). The spectra were used to confirm identities, extract the optimal fragment ions for SRM analysis and to obtain peptide retention times. MS^2 data were analyzed with the Mascot search engine (v. 2.1, MatrixScience) against a customized mouse Uniprot database (v. dated 07/2009) containing all the selected proteins and the corresponding decoy entries generated by inverting the amino-acid sequences of the tryptic peptides. Search parameters were set to 2.0 Da for the precursor mass tolerance, 0.8 Da for the fragment mass tolerance, fully tryptic peptides, no miscleavages and a false discovery rate (FDR) of 1% based on decoy assignments (Elias and Gygi, 2007). Cysteine carbamidomethylation was set to be a fixed modification, and methionine oxidation was used as a variable modification. A spectral library was generated from the validated fragment ion spectra using in-house written Perl scripts and for each

spectrum, the four most intense y-ions were selected as optimal SRM transitions to be monitored. Mass spectrometry parameters, such as collision energy and declustering potential, and further details in the generation of the peptide library, development of SRM assays and spectral library creation can be found in previous reports (Picotti *et al*, 2009, 2010).

Measurements and data analysis

SRM measurements were performed on a hybrid triple quadrupole/ion trap mass spectrometer (4000 Q-Trap, AB/Sciex) equipped with a nano-LC electrospray ionization source. Fused-silica microcapillary columns (75 µm) were pulled and packed with Magic C_{18} AQ 5 µm reverse-phase material (Michrom BioResources). Samples (2 µg) were loaded to a 2.5-cm pre-column (100 µm, New Objective) packed with C_{18} reverse-phase material and eluted with a linear gradient from 5% to 30% of buffer B in 30 min at a flow rate of 300 nl min^{-1} using a Tempo nanoLC system (Applied Biosystems, USA). Buffer A: 98% H_2O, 2% ACN and 0.1% formic acid; Buffer B: 2% H_2O, 98% ACN and 0.1% formic acid. Blank runs were performed between the SRM measurements of biological samples to avoid sample carryover. Measurements were done in scheduled SRM mode, using a retention time window of 5 min, *ca.* 400 transitions per method and a cycle time of 2.5 s, which ensured a dwell time over 10 ms per transition. Targeted peptides were only acquired in their corresponding OFFGEL fraction and three replicates for each time point were used in these measurements.

Transition groups corresponding to the targeted peptides were evaluated with MultiQuant v. 1.1 Beta (Applied Biosystems) based on different parameters (in order of importance): (i) co-elution of the transition traces associated with a targeted peptide, both in its light and heavy form; (ii) presence of at least four co-eluting transition traces for a given peptide exceeding a signal-to-noise ratio of 3; (iii) rank correlation between the light SRM relative intensities and the heavy counterparts; (iv) rank correlation between the SRM relative intensities and the intensities obtained in the MS^2 spectra during the SRM assay development; and (v) consistence among replicates.

Initially, all peak intensities were transformed by the logarithm based 2 and transitions with completely missing intensities in more than two thirds of the samples were removed. A constant normalization was applied to all measurements to equalize the median peak intensities of reference transitions between runs (Zien *et al*, 2001). The remaining normalized SRM peak intensities were retained for quantitative analysis. In summary, a set of 144 targeted proteins were observed and represented by 1–4 peptides each, and each peptide was represented by 2–4 pairs of light–heavy transitions.

Protein-level quantification and testing for differential abundance were performed using a linear mixed-effects model (McCulloch and Searle, 2001) as implemented in software package SRMstats (Chang *et al*, 2012). A list of *P*-values was calculated for each comparison, and was adjusted to control the FDR at a cutoff of 0.01 (Benjamini and Hochberg, 1995).

Raw data were deposited in the PASSEL repository with the data set identifier PASS00244.

Supplementary information

Supplementary information is available at the *Molecular Systems Biology* website (www.nature.com/msb).

Acknowledgements

Conflict of interest

The authors declare that they have no conflict of interest.

References

Almind K, Kahn CR (2004) Genetic determinants of energy expenditure and insulin resistance in diet-induced obesity in mice. *Diabetes* **53:** 3274–3285

Benjamini Y, Hochberg Y (1995) Controlling the false discovery rate: a practical and powerful approach to multiple testing. *J R Stat Soc Series B (Methodol)* **57:** 289–300

Bensimon A, Heck AJR, Aebersold R (2012) Mass spectrometry-based proteomics and network biology. *Annu Rev Biochem* **81:** 379–405

Biddinger SB, Almind K, Miyazaki M, Kokkotou E, Ntambi JM, Kahn CR (2005) Effects of diet and genetic background on sterol regulatory element-binding protein-1c, stearoyl-CoA desaturase 1, and the development of the metabolic syndrome. *Diabetes* **54:** 1314–1323

Cantó C, Gerhart-Hines Z, Feige JN, Lagouge M, Noriega L, Milne JC, Elliott PJ, Puigserver P, Auwerx J (2009) AMPK regulates energy expenditure by modulating NAD+ metabolism and SIRT1 activity. *Nature* **458:** 1056–1060

Chang C-Y, Picotti P, Hüttenhain R, Heinzelmann-Schwarz V, Jovanovic M, Aebersold R, Vitek O (2012) Protein significance analysis in selected reaction monitoring (SRM) measurements. *Mol Cell Proteomics* **11:** M111.014662

Costenoble R, Picotti P, Reiter L, Stallmach R, Heinemann M, Sauer U, Aebersold R (2011) Comprehensive quantitative analysis of central carbon and amino-acid metabolism in Saccharomyces cerevisiae under multiple conditions by targeted proteomics. *Mol Syst Biol* **7:** 464

Dephoure N, Gygi SP (2012) Hyperplexing: a method for higher-order multiplexed quantitative proteomics provides a map of the dynamic response to rapamycin in yeast. *Sci Signal* **5:** rs2

Desiere F, Deutsch EW, King NL, Nesvizhskii AI, Mallick P, Eng J, Chen S, Eddes J, Loevenich SN, Aebersold R (2006) The PeptideAtlas project. *Nucleic Acids Res* **34:** D655–D658

Dixon JB, Bhathal PS, Hughes NR, O'Brien PE (2004) Nonalcoholic fatty liver disease: Improvement in liver histological analysis with weight loss. *Hepatology* **39:** 1647–1654

Dixon JB, Bhathal PS, O'Brien PE (2001) Nonalcoholic fatty liver disease: predictors of nonalcoholic steatohepatitis and liver fibrosis in the severely obese. *Gastroenterology* **121:** 91–100

Domon B, Aebersold R (2006) Mass spectrometry and protein analysis. *Science* **312:** 212–217

Domon B, Aebersold R (2010) Options and considerations when selecting a quantitative proteomics strategy. *Nat Biotechnol* **28:** 710–721

Eckel RH, Alberti KG, Grundy SM, Zimmet PZ (2010) The metabolic syndrome. *Lancet* **375:** 181–183

Elias JE, Gygi SP (2007) Target-decoy search strategy for increased confidence in large-scale protein identifications by mass spectrometry. *Nat Methods* **4:** 207–214

Ideker T, Thorsson V, Ranish JA, Christmas R, Buhler J, Eng JK, Bumgarner R, Goodlett DR, Aebersold R, Hood L (2001) Integrated genomic and proteomic analyses of a systematically perturbed metabolic network. *Science* **292:** 929–934

Kirpich IA, Gobejishvili LN, Bon Homme M, Waigel S, Cave M, Arteel G, Barve SS, McClain CJ, Deaciuc IV (2011) Integrated hepatic transcriptome and proteome analysis of mice with high-fat diet-induced nonalcoholic fatty liver disease. *J Nutr Biochem* **22:** 38–45

Kulkarni RN, Almind K, Goren HJ, Winnay JN, Ueki K, Okada T, Kahn CR (2003) Impact of genetic background on development of hyperinsulinemia and diabetes in insulin receptor/insulin receptor substrate-1 double heterozygous mice. *Diabetes* **52:** 1528–1534

Lange V, Malmstrom JA, Didion J, King NL, Johansson BP, Schafer J, Rameseder J, Wong C-H, Deutsch EW, Brusniak M-Y, Buhlmann P, Bjorck L, Domon B, Aebersold R (2008) Targeted quantitative analysis of Streptococcus pyogenes virulence factors by multiple reaction monitoring. *Mol Cell Proteomics* **7:** 1489–1500

Luyckx FH, Lefebvre PJ, Scheen AJ (2000) Non-alcoholic steatohepatitis: association with obesity and insulin resistance, and influence of weight loss. *Diabetes Metab* **26:** 98–106

Mallick P, Schirle M, Chen SS, Flory MR, Lee H, Martin D, Ranish J, Raught B, Schmitt R, Werner T, Kuster B, Aebersold R (2007) Computational prediction of proteotypic peptides for quantitative proteomics. *Nat Biotechnol* **25:** 125–131

Marchesini G, Brizi M, Bianchi G, Tomassetti S, Bugianesi E, Lenzi M, McCullough AJ, Natale S, Forlani G, Melchionda N (2001) Nonalcoholic fatty liver disease: a feature of the metabolic syndrome. *Diabetes* **50:** 1844–1850

Martens L, Hermjakob H, Jones P, Adamski M, Taylor C, States D, Gevaert K, Vandekerckhove J, Apweiler R (2005) PRIDE: the proteomics identifications database. *Proteomics* **5:** 3537–3545

McCulloch CE, Searle SR (2001) *Generalized, Linear, and Mixed Models.* New York, NY, USA: John Wiley & Sons, Inc

Michalski A, Cox J, Mann M (2011) More than 100,000 detectable peptide species elute in single shotgun proteomics runs but the majority is inaccessible to data-dependent LC-MS/MS. *J Proteome Res* **10:** 1785–1793

Pagano G, Pacini G, Musso G, Gambino R, Mecca F, Depetris N, Cassader M, David E, Cavallo-Perin P, Rizzetto M (2002) Nonalcoholic steatohepatitis, insulin resistance, and metabolic syndrome: further evidence for an etiologic association. *Hepatology* **35:** 367–372

Park JY, Seong JK, Paik Y-K (2004) Proteomic analysis of diet-induced hypercholesterolemic mice. *Proteomics* **4:** 514–523

Picotti P, Bodenmiller B, Mueller LN, Domon B, Aebersold R (2009) Full dynamic range proteome analysis of S. cerevisiae by targeted proteomics. *Cell* **138:** 795–806

Picotti P, Rinner O, Stallmach R, Dautel F, Farrah T, Domon B, Wenschuh H, Aebersold R (2010) High-throughput generation of selected reaction-monitoring assays for proteins and proteomes. *Nat Methods* **7:** 43–46

Roberts CK, Sindhu KK (2009) Oxidative stress and metabolic syndrome. *Life Sci* **84:** 705–712

Sabido E, Quehenberger O, Shen Q, Chang C-Y, Shah I, Armando AM, Andreyev A, Vitek O, Dennis EA, Aebersold R (2012) Targeted proteomics of the eicosanoid biosynthetic pathway completes an integrated genomics-proteomics-metabolomics picture of cellular metabolism. *Mol Cell Proteomics* **11:** M111.014746

Schmid GM, Converset V, Walter N, Sennitt MV, Leung K-Y, Byers H, Ward M, Hochstrasser DF, Cawthorne MA, Sanchez J-C (2004) Effect of high-fat diet on the expression of proteins in muscle, adipose tissues, and liver of C57BL/6 mice. *Proteomics* **4:** 2270–2282

Schwanhäusser B, Busse D, Li N, Dittmar G, Schuchhardt J, Wolf J, Chen W, Selbach M (2011) Global quantification of mammalian gene expression control. *Nature* **473:** 337–342

Whaley-Connell A, McCullough PA, Sowers JR (2011) The role of oxidative stress in the metabolic syndrome. *Rev Cardiovasc Med* **12:** 21–29

Zien A, Aigner T, Zimmer R, Lengauer T (2001) Centralization: a new method for the normalization of gene expression data. *Bioinformatics* **17**(Suppl 1)**:** S323–S331